Purdue University
Purdue e-Pubs

International Compressor Engineering Conference

School of Mechanical Engineering

2016

Experimental Determination of Correlations for Heat Transfer Coefficients in the Suction Muffler of a Hermetic Reciprocating Compressor

Eduardo Arceno
POLO/Federal University of Santa Catarina, Brazil, earceno@yahoo.com.br

Thiago Dutra
POLO/Federal University of Santa Catarina, Brazil, dutra@polo.ufsc.br

Cesar Jose Deschamps
POLO/Federal University of Santa Catarina, Brazil, deschamps@polo.ufsc.br

Experimental Determination of Correlations for Heat Transfer Coefficients in the Suction Muffler of a Hermetic Reciprocating Compressor

Eduardo ARCENO, Thiago DUTRA, Cesar J DESCHAMPS*

POLO Research Laboratories for Emerging Technologies in Cooling and Thermophysics
Federal University of Santa Catarina
88040-900, Florianopolis, SC, Brazil
earceno@yahoo.com.br, dutra@polo.ufsc.br, deschamps@polo.ufsc.br

* Corresponding Author

ABSTRACT

The efficiency and reliability of hermetic reciprocating compressors adopted for household refrigeration are affected by the temperature distribution of their components. Simulation models developed to assist the thermal design of compressors require heat transfer coefficients in different components, usually estimated from correlations available for simplified geometries. However, the geometries of some components are complex and require more representative heat transfer coefficients. This paper presents experimental results for heat transfer coefficients obtained from measurements of heat flux and temperature in different regions of the suction muffler of a small reciprocating compressor under different operating conditions. A least square method was employed to obtain correlations for local heat transfer coefficients, which were then compared with estimates given by correlations available in the literature for simplified geometries.

1. INTRODUCTION

According to Ribas Jr. (2007), the suction gas superheating is responsible for half of the thermodynamic losses associated with the compression cycle of small reciprocating compressors. Such a superheating is a result of heat sources inside the compressor due to the compression process, electrical motor inneficiency and friction in bearings. Many studies have been carried out to better understand heat transfer between the compressor components. Todescat *et al*. (1992), Rigola *et al.* (2000) and Ooi (2003) proposed simulation models based on lumped formulations to predict the temperature distribution in reciprocating compressors. These models consist in applying energy balances to control volumes which encompass the compressor components, with heat transfer being modeled through heat conductances determined from experimental data or simplified correlations available in the literature.

Chikurde *et al.* (2002), Raja (2003) and Birari *et al*. (2006) carried out three-dimensional simulations of heat conduction and fluid flow in compressors using commercial softwares. Although these models allow a more detailed thermal characterization of the compressor, they are time-consuming and not viable for optimization purpose. Ribas (2007) and Sanvezzo Jr. and Deschamps (2012) circumvented this difficulty of computational cost by proposing the so-called hybrid model in which the benefit of solving heat conduction with a three-dimensional formulation is maintained, but a lumped formulation is adopted for the fluid flow domain. The hybrid model developed by Sanvezzo Jr. and Deschamps (2012) estimates heat transfer at the interface between solid and fluid through convective heat transfer coefficients obtained from the literature.

Heat transfer in reciprocating compressors has also been experimentally investigated (Meyer and Thompson, 1990; Kim *et al.*, 2000), adopting thermocouples to measure the temperature of the gas in different locations. By combining these measurements with energy balances, heat transfer rates for compressor components were determined. Shiva Prasad (1992) carried out instantaneous heat flux measurements in the compression chamber of a 900 rpm air compressor by employing thin-film heat flux sensors (HFSs), with the main objective of analyzing the influence of the regenerative heat transfer on the suction gas superheating. Recently, Dutra and Deschamps (2013) adopted HFSs and thermocouples to measure heat flux at the surfaces of components and estimate local heat transfer coefficients. The authors carried out measurements in the compressor shell, electrical motor, discharge chamber and suction muffler of a single-speed reciprocating compressor and concluded that the lubricant oil flow greatly affects heat transfer inside the compressor and that the local heat transfer coefficients are almost insensitive to evaporating and condensing temperatures.

The present paper reports an experimental characterization of heat transfer coefficients at different locations of the suction muffler of a variable-speed reciprocating compressor. Measurements are carried out for three compressor speeds (1200, 2000 and 4000 rpm) and three pairs of evaporating and condensing temperatures (-15°C/40°C; -25°C/40°C and -25°C/55°C). Based on such measurements, a least square method is employed to obtain correlations for local heat transfer coefficients, which are then compared with estimates of correlations available in the literature for simplified geometries.

2. EXPERIMENTAL PROCEDURE

2.1 Compressor Instrumentation

The suction muffler considered in this work is composed by two independent parts, herein called front and back parts, forming an array of three tubes and two chambers, as depicted in Figure 1. The refrigerant gas enters the muffler through tube 1, being then released into the chamber 1. The gas is then driven to the chamber 2 by flowing in the tube 2. Finally, the gas flows towards the compression chamber through tube 3.

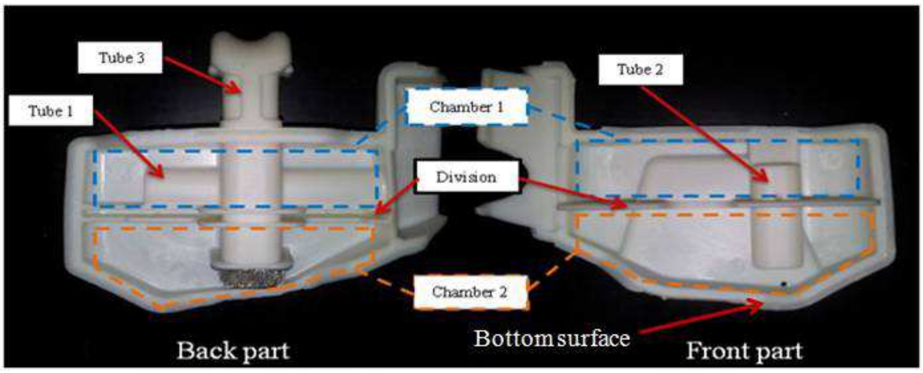

Figure 1: Suction muffler regions.

Six samples of this suction muffler geometry were employed in this study. Three of them, named as group A, were instrumented only with thermocouples and the other three, group B, were instrumented with thermocouples and HFSs. Mufflers of group A were instrumented with thermocouples on their external surfaces (Figure 2) and in convenient positions along the suction path (Figure 3).

Two HFSs were installed in each sample of suction muffler of group B, one positioned on the front wall and the other on the back wall (Figure 4). The working principle of a HFS is based on a self-generated voltage output which is proportional to the heat flux that crosses the sensor. The relationship between output voltage, E, and heat flux, q'', is represented by a linear function ($q'' = E / S$), where S is the sensitivity associated to a specific HFS. The HFS sensitivity is obtained from a calibration procedure and its value is usually specified by the manufacturer. Further details regarding the HFS working principle are available in Dutra and Deschamps (2013).

The HFSs have to be carefully fitted onto the suction muffler walls. Due to the presence of lubricating oil at high temperature inside the compressor, an epoxy-adhesive was used to attach the HFSs to the surfaces. A thin layer of epoxy-adhesive was applied between the HFS and the muffler wall to reduce the contact resistance. This thin layer was thoroughly spread all over the HFS surface for preventing air bubbles from being formed between the sensor and the wall during the fitting process.

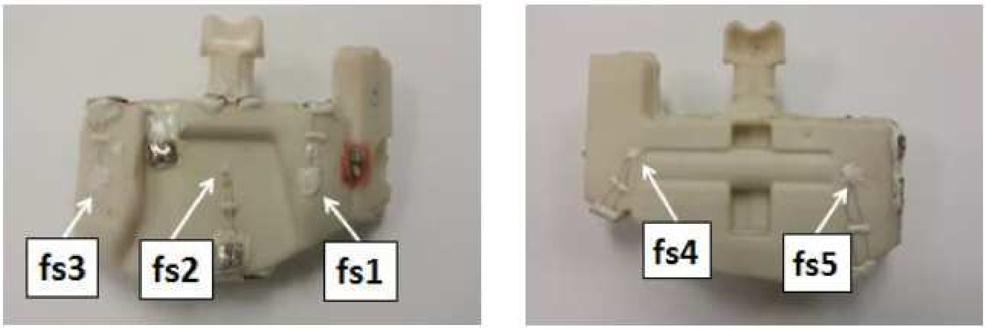

(a) (b)

Figure 2: Thermocouples (fs1 to fs5) located on the (a) front and (b) back surfaces of mufflers of group A.

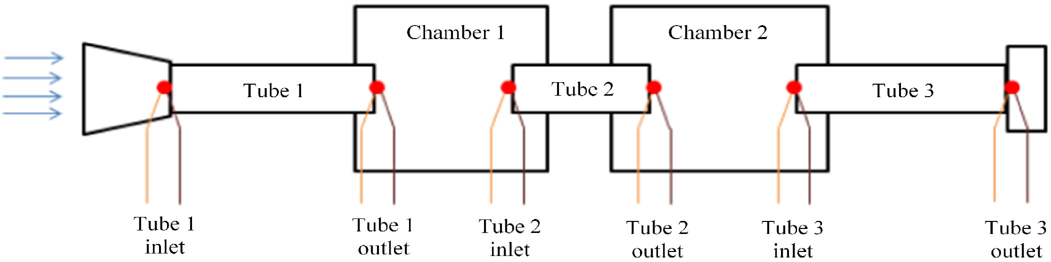

Figure 3: Schematic of the array of tubes and chambers and locations of thermocouples (groups A and B).

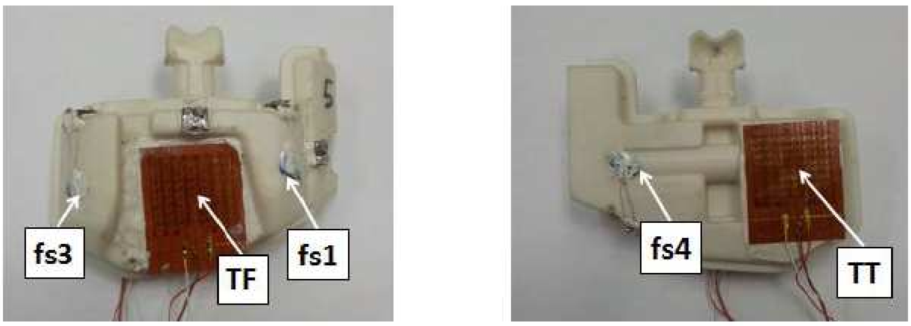

(a) (b)

Figure 4: Thermocouples (fs1, fs3 and fs4) and heat flux sensors (TF and TT) on the (a) front and (b) back surfaces mufflers of group B.

Four thermocouples were installed inside the compressor for measurements of temperature in convenient positions near the muffler external surface. Three of them were positioned near the front surface of the muffler to measure the gas temperature (Ci1, Ci2 and Ci3). The other thermocouple (tc) was installed onto the surface of the electrical motor that is 2 mm apart from the back surface of the muffler. Figure 5 shows a schematic view of the internal components of the compressor, highlighting the locations of the HFSs and thermocouples.

From the temperature measurements in the muffler vicinity, it was possible to establish the reference temperatures, T_∞, to estimate local heat transfer coefficients at the suction muffler surfaces:

$$h = \frac{q"}{T_s - T_\infty} \tag{1}$$

where T_s is the surface temperature measured by a thermocouple in the HFS and q'' is the heat flux measured with the HFS.

2.1 Experimental Facility

The compressor was tested in a calorimeter facility specially designed to establish and control different operating conditions. Figure 6 depicts a schematic of the calorimeter, which is composed of pipelines, control valves (CV), a mass flow meter (FM), heat exchangers (HX), a thermocouple (TC) and pressure transducers (PT). The compressor (C) raises the refrigerant pressure from point 1 up to point 2, which is then cooled by the heat exchanger HX1 at point 3. The refrigerant is then adiabatically throttled to an intermediate pressure level (point 4) by means of a control valve (CV1). A Coriolis mass flow meter (FM) measures the mass flow rate of refrigerant before it is cooled again with another heat exchanger (HX2), reaching point 5. A second expansion device (CV2) takes the refrigerant fluid to the evaporating pressure (point 6). Finally, an electrical heater (EH1) and a thermocouple (TC1) are used to adjust the temperature of the compressor suction line to the required gas superheating condition (point 1), completing the operating cycle.

The first step in experiments is to submit the compressor and the calorimeter pipeline to an adequate vacuum condition, so as to remove air and humidity. Then, a charge of refrigerant is supplied to the system, the operating condition is set and the compressor is switched on. A period of approximately 4 hours is needed until the compressor achieves a thermal stabilized condition. During this process, the control valves in the high and low pressure lines are continuously adjusted to establish the specified suction and discharge pressures within 1% of the set points. The compressor is considered to have reached the steady-state condition when the temperatures at several locations of the compressor vary less than 1°C in one hour. After that, samples of local temperature and heat flux measurements are acquired over a period of 15 minutes.

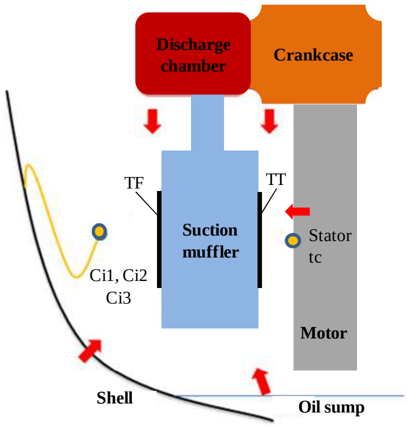

Figure 5: Locations of thermocouples and HFS inside the compressor.

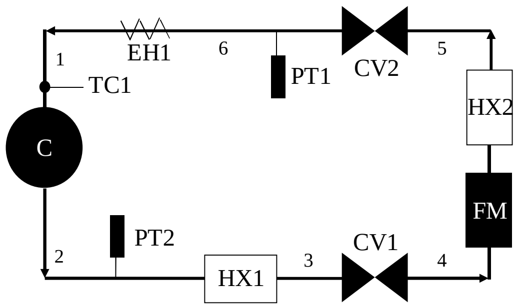

Figure 6: Schematic of the calorimeter facility.

3. RESULTS AND DISCUSSIONS

A variable-speed reciprocating compressor operating with R600a was selected for the analysis. The compressor was tested under three rotational speeds (1200, 2000 and 4000 rpm) and three operating conditions represented by different evaporating and condensing temperatures (T_e, T_c): A (-15°C, 40°C), B (-25°C, 40°C) and C (-25°C, 55°C), corresponding to pressure ratios, $\pi = p_c/p_e = 6.0$, 9.1 and 13.3. Considering that six samples of suction mufflers were employed in the experimental investigation, a total of 54 tests were carried out, providing mean values of local heat transfer coefficients. Such coefficients were made non-dimensional by dividing them by the coefficient h_{shell} associated with convection heat transfer between the shell and the calorimeter environment, i.e. $h^* = h/h_{shell}$, with $15 W.m^{-2}K^{-1} < h_{shell} < 30 W.m^{-2}K^{-1}$.

3.1 Measurements of Heat Transfer Coefficients

Mean values of heat flux and temperature measured at each surface were adopted to estimate the heat transfer coefficients. The reference temperature, T_∞, for the front surface was taken as the average of the values indicated by the thermocouples Ci1, Ci2 and Ci3 (Figure 5). On the other hand, the mean value of temperatures on the motor and muffler back surface was considered as the reference temperature to estimate the heat transfer coefficient on the back surface.

Figures 7 and 8 present results of heat transfer coefficients for the front, h_f^*, and back surfaces, h_b^*, of the suction muffler as a function of pressure ratio. As can be seen, the heat transfer coefficient increases with the compressor speed but decreases with the pressure ratio in most conditions. This is an expected behavior since the increase of speed or the decrease of pressure ratio provide higher mass flow rates for the operating conditions A, B and C, and, therefore, an intensification of the convective heat transfer. It is interesting to note that the heat transfer coefficient on the muffler front surface for the compressor operating at 2000 rpm slightly decreases from $\pi = 6.0$ to $\pi = 9.1$ and then increases as the pressure ratio rises to $\pi = 13.3$. Such a behavior is not trivial but may be related to variation of the lubricant oil flow path inside the compressor.

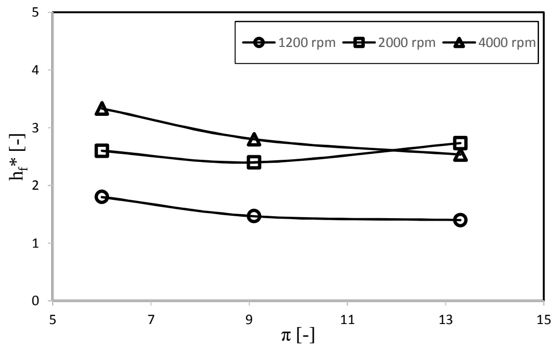

Figure 7: Heat transfer coefficients on the front surface of the suction muffler.

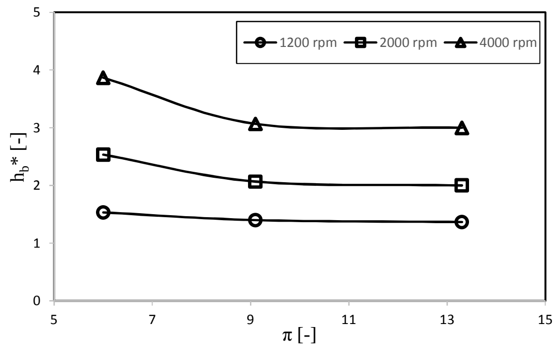

Figure 8: Heat transfer coefficients on the back surface of the suction muffler.

Heat transfer coefficients for the internal fluid flow through tubes and chambers of the muffler are obtained by combining measurements of temperature and heat flux with the hypothesis of one-dimensional heat transfer through the wall:

$$h = \frac{q''k}{k(\bar{T}_{se} - \bar{T}_\infty) - q''L} \tag{2}$$

where k and L are the thermal conductivity and thickness of the suction muffler wall, $\bar{T}_{se}$ is the mean temperature of the external surface and $\bar{T}_\infty$ is the mean temperature of the gas in the component under analysis (tube or chamber).

Tubes 1 and 2 are connected to the back and front surfaces of the muffler, respectively, as shown in Figure 1. Hence, heat flux measurements on these surfaces are used to estimate the local heat transfer coefficients, h, for tubes 1 and 2. This is certainly an approximation that will be verified in future work via energy balance and measurements of temperatures at the inlet and outlet of each tube. The heat transfer coefficient is not evaluated for the tube 3 because a considerable part of this tube is in contact with hot components of the cylinder head. Therefore, the hypothesis of one-dimensional heat transfer would not be applicable to tube 3. Figures 9 and 10 show the results of local heat transfer coefficients, h^*, for the tubes 1 and 2, respectively. Although such heat transfer coefficients are higher than those associated with the muffler external surfaces, their variations with compressor speed and pressure ratio are similar.

The determination of the heat transfer coefficients for the chambers followed a different procedure, since the temperature inside them is affected by heat fluxes through the front and back surfaces. Thus, a mean value of these heat fluxes was used to calculate the local heat transfer coefficients of both chambers, shown in Figures 11 and 12. The values of h^* for chamber 1 present the same levels and trends compared with those measured in the tubes.

However, the values of h^* for chamber 2 are higher than those observed for chamber 1 and show no clear relationship with both the pressure ratio and the compressor speed. This is arguably related to the more complex geometry of chamber 2, which gives rise to large recirculating flow regions inside the chamber that are less sensitive to the mass flow rate. Numerical simulations could assist clarifying this issue.

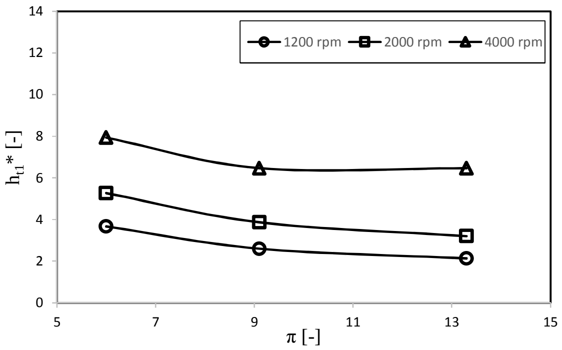

Figure 9: Heat transfer coefficients for tube 1.

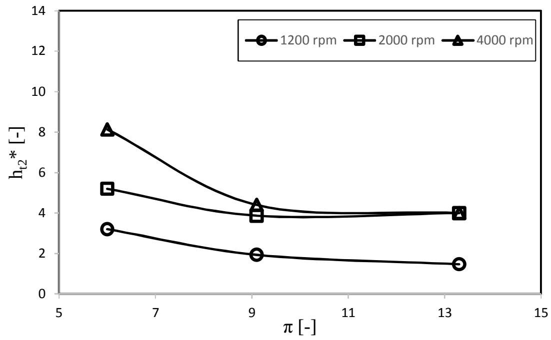

Figure 10: Heat transfer coefficients for tube 2.

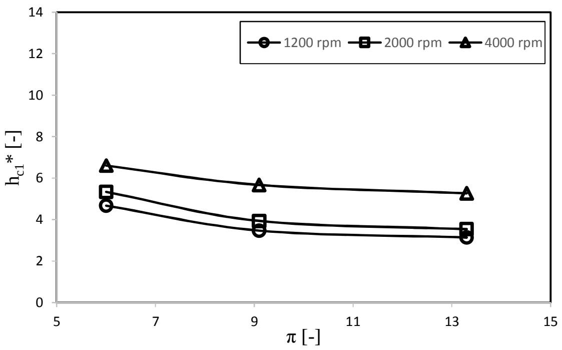

Figure 11: Heat transfer coefficients for chamber 1.

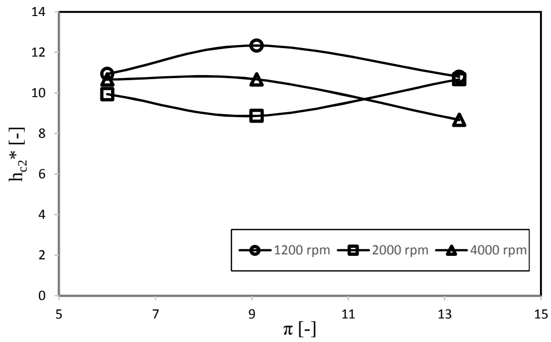

Figure 12: Heat transfer coefficients for chamber 2.

3.2 Heat Transfer Correlations

Heat transfer correlations for the suction muffler are usually expressed through the Nusselt number, Nu, as a function of the Reynolds number, Re, and Prandtl number, Pr, as defined in Equation (3):

$$Nu = \frac{hD}{k_f} \qquad Re = \frac{VD}{\nu} \qquad Pr = \frac{\nu}{\alpha} \tag{3}$$

where ν, α, k_f are the kinematic viscosity, thermal diffusivity and thermal conductivity of the refrigerant gas, respectively, V is the characteristic velocity and D is the characteristic length of the phenomenon. The Prandtl number was found to have a small effect on the Nusselt number for the range of operating conditions tested in our study and, hence, was not included in the heat transfer correlation. Modified expressions for the Nusselt and Reynolds numbers can be written by dividing their original expressions by the characteristic length, D:

$$Re^* = \frac{Re}{D} = \frac{V}{\nu} \qquad Nu^* = \frac{Nu}{D} = \frac{h}{k_f} \tag{4}$$

3.2.1 External surface: The Reynolds number for the external surfaces of the suction muffler was calculated by adopting the crankshaft tangential velocity as the characteristic velocity, V, since its rotational motion promotes the gas flow inside the shell, and as a consequence, around the suction muffler. The Nusselt number was estimated for each operating condition by averaging the heat transfer coefficients measured on the front and back surfaces. Fluid properties were evaluated by using the film temperature.

Reynolds and Nusselt numbers, Re^* and Nu^*, as a function of the compressor speed and pressure ratio are shown in Figures 13 and 14. Both parameters are seen to increase with the compressor speed. The Reynolds number dependence on compressor speed is directly related to the crankshaft tangential velocity. Moreover, the increase of the crankshaft tangential velocity intensifies the flow of gas and oil inside the compressor shell, increasing heat transfer and the Nusselt number. On the other hand, both parameters are found to increase as the pressure ratio decreases. Actually, this dependence on pressure ratio is associated with the evaporating pressure, because both Reynolds and Nusselt numbers vary as π moves from 6.0 (-15°C/40°C) to 9.1 (-25°C/40°C), but remain roughly constant when π changes from 9.1 to 13.3 (-25°C/55°C). In fact, the density of the gas in the suction muffler increases with the evaporating pressure, and hence increasing the Reynolds number and Nusselt number.

Experimental data and two correlations for the Nusselt number as a function of the Reynolds number are shown in Figure 15. Measurements are presented with uncertainty bars corresponding to a 95% confidence interval. A least square method was employed to fit a logarithm function to these measurements:

$$Nu^* = 9.56 \times 10^2 \ln(Re^*) - 1.06 \times 10^4 \tag{5}$$

which is valid for $2\text{x}10^5 \leq Re^* \leq 10^6$. The determination coefficient, R^2, is 0.94, indicating that the fitted curve is reasonably correlated with the experimental data. For the purpose of comparison, the curve associated with heat transfer correlation for the flow past a sphere (Whitaker, 1972) is also shown in Figure 15. The good agreement observed between both correlations suggests that a correlation for sphere could be used to estimate heat transfer on the external surfaces of suction mufflers.

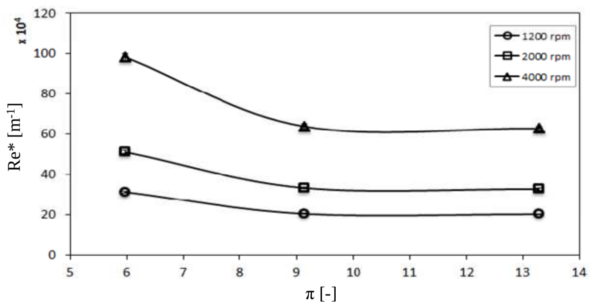

Figure 13: Reynolds number for the external surface of the suction muffler.

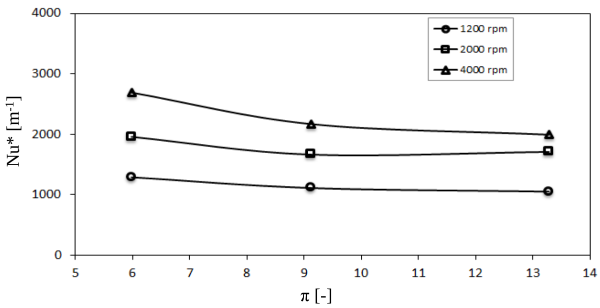

Figure 14: Nusselt number for the external surface of the suction muffler.

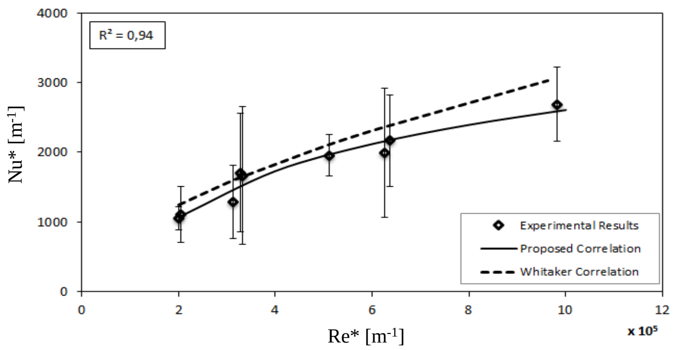

Figure 15: Comparison between correlations at the external surface.

3.2.2 Tubes: The characteristic velocity V necessary to define the Reynolds number is obtained from the mass flow rate, $\dot{m}$, the tube diameter, D, and the gas density in the tube, ρ, ($V = 4\dot{m}/\rho\pi D^2$). Nusselt numbers are evaluated from the heat transfer coefficients presented in Figures 9 and 10.

Figure 16 shows experimental data for Nusselt number as a function of the Reynolds number for tubes1 and 2. As expected, the Nusselt number increases with the Reynolds number for both tubes. Moreover, the results are similar for tube 1 and 2, especially for low Reynolds numbers. A heat transfer correlation for the flow in the suction muffler tubes is proposed by the following logarithm expression:

$$Nu^{*} = 2.46 \times 10^{3} \ln(Re^{*}) - 3.12 \times 10^{4} \quad (6)$$

for a range of $5\text{x}10^5 \leq Re^* \leq 3.5\text{x}10^6$. Figure 17 shows the fitted curve (R^2= 0.85), with a maximum deviation of 34% between measurements and values given by the correlation. Figure 17 shows a comparison between the experimental data and estimates for Nusselt number in the tubes 1 and 2, given by Equation (6) and the correlations for tubes developed by Dittus and Boelter (1930) and Gnielinski (1976). There is a good agreement between the three correlations for $Re^* < 1.8\text{x}10^6$. In the situations of high Reynolds numbers, the estimates from the literature correlations overpredict the heat transfer in the tubes.

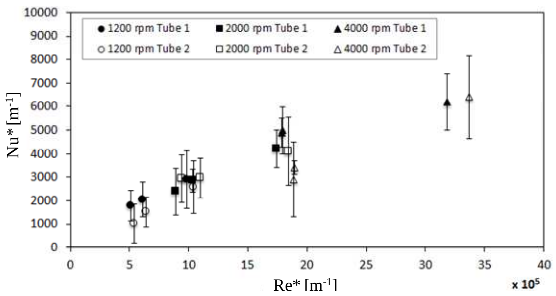

Figure 16: Nusselt number for tubes 1 and 2 as a function of Reynolds number.

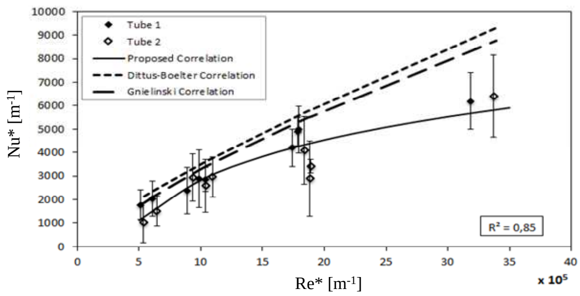

Figure 17: Comparison between estimates for Nusselt number given by different correlations for tubes.

3.2.3 Chambers: The specification of the characteristic velocity V in the chambers is a difficult task, due to the flow geometry complexity. For chamber 1, a hydraulic diameter was defined by using the perimeter of the chamber cross-sectional area immediately after the outlet of tube 1. For chamber 2, the distance between the outlet of tube 2 and the bottom surface of chamber 2 (Figure 1) was adopted as the hydraulic diameter. The characteristic velocity was then evaluated as $V = 4\dot{m}/\rho\pi D_h^2$. The Nusselt numbers are assessed from the heat transfer coefficients presented in Figures 11 and 12.

Figure 18 shows values of Nusselt number for different Reynolds numbers in chambers 1 and 2. The results for chamber 1 are similar to those observed in the tubes. On the other hand, as a consequence of the results shown in Figure 12, there is no clear relationship between Nu^* and Re^* for chamber 2.

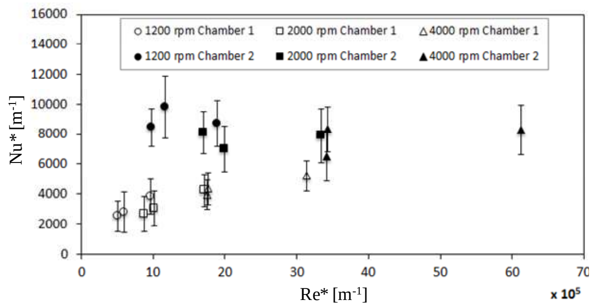

Figure 18: Nusseltnumber for chambers 1 and 2.

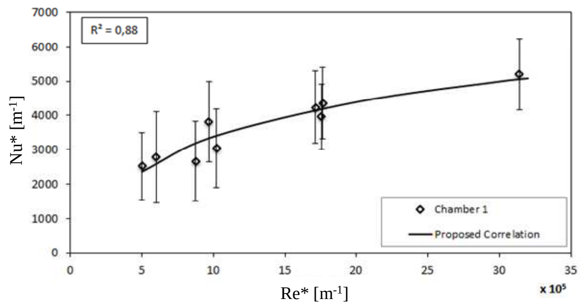

Figure 19: Nusselt correlation for chamber 1.

Since no variation was observed for the Nusselt number in the chamber 2 for different Reynolds numbers, a heat transfer correlation is only proposed for chamber 1,

$$Nu^{*} = 1.47 \times 10^{3} \ln(Re^{*}) - 1.69 \times 10^{4} \quad (7)$$

considering $5x10^5 \leq Re^* \leq 3.2x10^6$. As observed in Figure 19, reasonable fitting was achieved ($R^2 = 0.88$) and the maximum deviation between the experimental data and correlation is about 27%.

4. CONCLUSIONS

An experimental study of heat transfer in the suction muffler of a variable-speed hermetic reciprocating compressor was carried out. Measurements of temperature and heat flux were carried out in different locations of the suction muffler. Heat transfer coefficients were obtained from such measurements at the external surface of the suction muffler as well as in internal tubes and chambers. Local heat transfer coefficients were found to increase with the compressor speed and evaporating pressure for most of the suction muffler regions. Heat transfer correlations were developed based on the measurements and compared with those available in the literature for simplified geometries. The correlation proposed herein for heat transfer on the external surface of the suction muffler was in good agreement with that obtained by Whitaker (1972) for heat transfer of flow past a sphere. For the suction muffler tubes, the classical correlations of Dittus and Boelter (1930) and Gnielinski (1976) were found to reasonably predict heat transfer for low Reynolds numbers.

NOMENCLATURE

D	characteristic length	(m)	p_e	evaporating pressure	(Pa)
D_h	hydraulic diameter	(m)	q''	heat flux	($W.m^{-2}$)
h	heat transfer coefficient	($W.m^{-2}.K^{-1}$)	Re	Reynolds number	(-)
h^*	non-dimensional heat transfer coefficient	(-)	Re*	modified Reynolds number	(m^{-1})
h_{shell}	heat transfer coefficient at the compressor shell	($W.m^{-2}.K^{-1}$)	T_s	surface temperature	(K)
k	muffler thermal conductivity	($W.m^{-1}.K^{-1}$)	T_∞	reference temperature	(K)
k_f	gas thermal conductivity	($W.m^{-1}.K^{-1}$)	V	characteristic flow velocity	($m.s^{-1}$)
L	muffler wall thickness	(m)	α	thermal diffusivity	($m^2.s^{-1}$)
$\dot{m}$	mass flow rate	($kg.s^{-1}$)	ν	gas kinematic viscosity	($m^2.s^{-1}$)
Nu	Nusselt number	(-)	π	pressure ratio	(-)
Nu*	modified Nusseld number	(m^{-1})	ρ	gas density	($kg.m^{-3}$)
p_c	condensing pressure	(Pa)			

REFERENCES

Birari, Y. V., Gosavi, S. S., Jorwekar, P. P., 2006, Use of CFD in design and development of R404a reciprocating compressor, *Proc. Int. Compressor Engrg. Conf. at Purdue*, paper C072.

Cavallini, A., Doretti, L., Longo, G. A., Rosseto, L., Bella, B., Zannerio, A., 1996, Thermal analysis of a hermetic reciprocating compressor, *Proc. Int. Compressor Engrg. Conf. at Purdue*, pp. 535- 540.

Chikurde, R. C., Loganathan, E., Dandekar, D. P., Manivasagam, S., 2002, Thermal mapping of hermetically sealed compressors using computational fluid dynamics technique, *Proc. Int. Compressor Engrg. Conf. at Purdue*, paper C6-4.

Dittus, F. W., Boelter, L. M. K., 1930, Heat transfer in automobile radiators of the tubular type, *Berkeley Publ. Eng.* 2, Univ. California, pp. 443–461.

Dutra, T., Deschamps, C. J., 2013, Experimental characterization of the heat transfer in the components of a small hermetic reciprocating compressor, *App. Thermal Engrg.* 58, pp. 499-510.

Gnielinski, V., 1976, New equations for heat and mass transfer in turbulent pipe and channel flow, *Int. Chemical Engrg*, 16 (2), pp. 359–368.

Kim, S. H., Sim, Y. H., Youn, Y., Min, M. K., 2000, An experimental study on internal temperature cistribution and performance characteristics in a reciprocating compressor for a domestic refrigerator, *Proc. Int. Compressor Engrg. Conf. at Purdue*, pp. 245-252.

Meyer, W. A., Thompson, H. D., 1990, An analytical model of heat transfer to the suction gas in a Low-Side hermetic refrigeration compressor, *Proc. Int. Compressor Engrg. Conf. at Purdue*, pp. 898-907.

Ooi, K. T., 2003, Heat transfer study of a hermetic refrigeration compressor, *App. Thermal Engrg*., 23, pp. 1931 – 1945.

Raja, B., Sekhar, S. J., Lal, D. M., Kalanidhi, A., 2003, A numerical model for thermal mapping in a hermetically sealed reciprocating refrigerant compressor, *Int. J. of Refrigeration 26 (6)*, pp. 229-236.

Ribas Jr., F. A., 2007, Thermal analysis of reciprocating compressors, *Int. Conf. on Compressors and Their Systems*, London, pp. 277-287.

Rigola, J., Pérez-Segarra, C. D., Oliva, A., 2000, Advanced numerical simulation model of hermetic reciprocating compressors. Parametric study and detailed experimental validation, *Proc. Int. Compressor Engrg. Conf. at Purdue,* pp. 23-30.

Sanvezzo Jr., J., Deschamps, C. J., 2012, A heat transfer model combining differential and integral formulations for thermal analysis of reciprocating compressors, *Proc. Int. Compressor Engrg. Conf. at Purdue*, paper 1343.

Shiva Prasad, B. G., 1992. Regenerative heat transfer in reciprocating compressors, based on the paper presented at *PCRC Int. Reciprocating Machinery Conf. at Denver/USA.*

Todescat, M. L., Fagotti, F., Prata, A.T., Ferreira, R.T.S., 1992, Thermal energy analysis in reciprocating hermetic compressors, *Proc. Int. Compressor Engrg. Conf. at Purdue*, pp. 1417-1428.

Whitaker, S., 1972, Forced convection heat transfer correlations for flow in pipes, past flat plates, single cylinders, single spheres, and for flow in packed beds and tube bundles, *AlChE J.*, 18 (2), pp. 361–371.

ACKNOWLEDGEMENT

This study is part of a technical-scientific program between the Federal University of Santa Catarina and EMBRACO. Financial support from EMBRAPII Unit POLO/UFSC and CNPq (Brazilian Research Council) is also acknowledged.